

Infrared Multiple-Photon Decomposition of Cyclopentene

James O. Shoemaker and Robert W. Carr, Jr.*

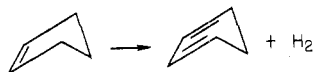
Department of Chemical Engineering and Materials Science, University of Minnesota, Minneapolis, Minnesota 55455 (Received: May 25, 1983)

The infrared multiple-photon decomposition of cyclopentene yields cyclopentadiene as the major hydrocarbon product (>95%). The other products are 1,4-pentadiene and *cis*- and *trans*-1,3-pentadiene, along with trace amounts of fragmentation products. The 1,3-pentadienes have not been previously reported in cyclopentene pyrolysis. Typical conversions obtained by focussing the laser beam into the sample ranged from less than 1% to as much as 20% per 10^3 pulses with estimated beam waist fluences of approximately 150 J/cm^2 , indicating that cyclopentene excitation is strongly bottlenecked. No products were detected with collimated beams of 1 J/cm^2 and after 1.7×10^4 pulses. Reaction product yields increase with increasing wavelength in the fundamental absorption band centered at 1048 cm^{-1} . Excitation originating in the Q branch of this transition results in very small yields. Total C_5 yields increase rapidly with increasing fluence at 1029 and 1033 cm^{-1} . A simple model of dissociation in which the focused beam geometry is a circular hyperboloid of revolution predicts fluence-yield behavior that is consistent with experimental observations. Conversion of cyclopentene decreases with increasing cyclopentene pressure between 0.01 and about 0.5 torr, and thereafter increases rapidly with increasing pressure. On the other hand, addition of N_2 , up to about 200 torr, causes total C_5 yields to decrease monotonically over the entire pressure range. A limited number of experiments were done with 1-methylcyclopentene. At the same wavelength (1019 cm^{-1}), pressure, fluence, and weak field absorbance, dehydrogenation of 1-methylcyclopentene gives yields that are as much as 20 times greater than yields from cyclopentene.

Introduction

High-power infrared lasers can be used to induce unimolecular reactions in polyatomic molecules by multiple-photon excitation to energies greater than the reaction threshold. Unimolecular processes that have been observed include bond dissociations, molecular eliminations, and isomerizations. In this paper we report a study of the infrared multiple-photon decomposition (IRMPD) of cyclopentene, which has not previously been reported.

Cyclopentene is an excellent candidate for IRMPD studies. The thermal decomposition has been extensively studied, and the Arrhenius activation energy and preexponential factor are reliably known.¹ The major thermal reaction channel is unimolecular H_2 elimination to yield cyclopentadiene.



Cyclopentene has an infrared fundamental absorption band at 1048 cm^{-1} and a weaker band at about 975 cm^{-1} , both of which can be excited by CO_2 laser lines. Furthermore, the 1048-cm^{-1} band falls on a window in the cyclopentadiene infrared absorption spectrum. Detailed analyses of the cyclopentene vibrational spectrum are available,^{2,3} showing that the 1048-cm^{-1} band corresponds to CH_2 motions that may lead directly to the transition state for 3,5 elimination of H_2 , the dominant thermal reaction path.⁷

Although the purpose of the initial study was to characterize the reaction products and the effects of experimental parameters on the product yield, cyclopentene provides an opportunity to study some interesting features of IRMPD. The dominant products of infrared laser-induced reactions usually come from the lowest energy reaction channel of the ground electronic state. Thus cyclopentadiene and hydrogen are the expected products from cyclopentene. It was of interest to see whether pumping the CH_2 motion of 1048 cm^{-1} would facilitate hydrogen elimination.

Although cyclopentene is a relatively large organic molecule which might be expected to have a reasonably high reaction probability per pulse, it is also a relatively stiff molecule. The results suggest that, in spite of its size, cyclopentene requires large laser energies to obtain reasonable yields per pulse, and that pumping the vibrations corresponding to the reaction coordinate provides no advantage. That vibrational state density is a strong influence on yield is corroborated by experiments with 1-methylcyclopentene.

It was also of interest to see if higher energy reaction channels that are not competitive with H_2 elimination by thermal excitation are accessible by infrared laser excitation. Multiple-channel reactions are well-known in IRMPD. The *cis*- and *trans*-1,3-pentadienes found here have not been reported in any of the thermal work to date.

Experimental Section

The radiation from a Lumonics 101-2 grating tuned TEA pulsed CO_2 laser, operated multimode, was passed through a circular aperture of 1.99-cm^2 area. The laser energy was calibrated with a Scientech 36-001 disk calorimeter and Model 362 power/energy meter. During experiments pulses were counted and integrated by electronics of our own design which are discussed elsewhere.⁴ The fluence per pulse which passed through the aperture ranged from about 0.4 to about 1.0 J/cm^2 for the P_{38} line of the $9\text{-}\mu\text{m}$ band at 1029 cm^{-1} , which was the primary line used to irradiate cyclopentene. Laser pulse energies in this paper are reported as fluences (J/cm^2) before focusing. Fluences at the focus were estimated to be at least 100 J/cm^2 . The laser radiation was focused by a 40-cm focal length ZnSe lens through the center of a $2.5 \text{ cm} \times 30 \text{ cm}$ Pyrex reaction cell with NaCl or KCl windows, and greaseless glass-teflon vacuum valves. The cells were placed such that the focal point of the lens was at midpoint on the centerline of the cell. The beam diameter at the windows was then about 0.5 cm. No visible luminescence was observed with a dark-adapted eye either from the laser beam hitting the cell window or the cell volume itself in any experiment. Light absorption measurements were carried out on the evacuated cells and the lens itself to allow back-calculation of fluence entering the cell from measurements made of fluence leaving the cell.

A conventional glass vacuum system with a mercury diffusion pump was used for sample preparation. Chemical Samples Co.

(1) (a) D. W. Vanas and W. D. Walters, *J. Am. Chem. Soc.*, **70**, 4035 (1948); (b) G. I. Mackay and R. E. March, *Can. J. Chem.*, **48**, 913 (1970); (c) D. A. Knecht, *J. Am. Chem. Soc.*, **95**, 7933 (1973); (d) K. O. King, *Int. J. Chem. Kinet.*, **10**, 117 (1978).

(2) L. M. Sverdlov and E. N. Krainov, *Opt. Spectrosc. (USSR)*, **6**, 214 (1959).

(3) J. R. Villarreal, J. Laane, S. F. Bush, and W. C. Harris, *Spectrochim. Acta, Part A*, **35**, 311 (1979).

(4) J. O. Shoemaker and R. W. Carr, Jr., *Rev. Sci. Instrum.*, **53**, 1086 (1982).

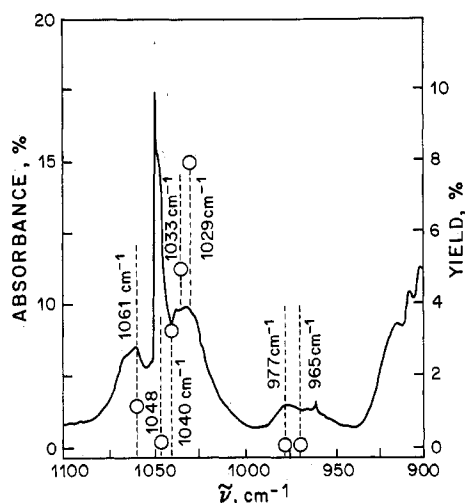


Figure 1. Solid line, infrared spectrum of cyclopentene, $p = 10.65$ torr; O, C_5 product yield per 10^3 pulses at 0.6 J/cm^2 .

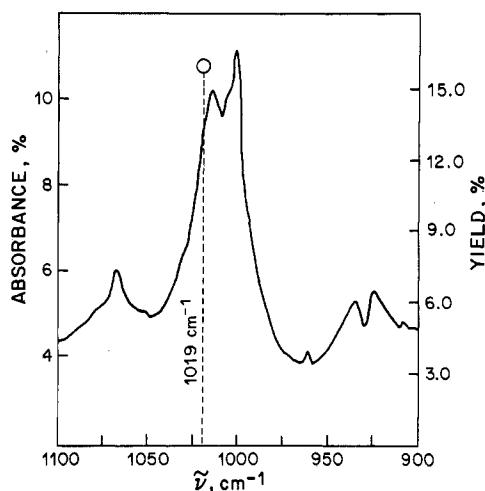


Figure 2. Solid line, infrared spectrum of 1-methylcyclopentene, $p = 10.65$ torr; O, C_6 product yield per 10^3 pulses at 0.6 J/cm^2 .

cyclopentene (99.9%) was used without further purification and degassed, as were all liquid samples, by a freeze-pump-thaw technique and then stored at room temperature under its own vapor. Vapor was withdrawn as needed. Chemical Samples Co. dicyclopentadiene (99%) was distilled to cyclopentadiene.⁵ Fresh distillate was always degassed and used at once. Aldrich Chemical Co. 1-methyl-1-cyclopentene (96%) was prepared, stored, and then used in the same manner as cyclopentene. Pressure in the prepared cell was measured with an MKS Baratron Type 222 0–10-torr pressure transducer with a digital display accurate to 1 mtorr. In experiments including a nitrogen bath gas a measured pressure of the cyclopentene was condensed into a cold finger and isolated. After evacuation the desired pressure of nitrogen was introduced. The system was reisolated and the cyclopentene allowed to interdiffuse with the nitrogen in the cell.

After irradiation, typically 1000 laser pulses, the cell was pressurized with ambient air by momentarily opening the valve. The gaseous products were analyzed with a Hewlett-Packard 5730A gas chromatograph using a flame ionization detector and Hewlett-Packard 3390A reporting integrator. Usually three or four analyses were obtained from a single experiment. The column used was a 2-m, $1/8$ -in. o.d. aluminum tube packed with 20 wt% dimethylsulfolane on 60/80 chromosorb. It was assumed that all the C_5 products had the same fid response. The relative response of the fid to cyclopentene and cyclopentadiene was

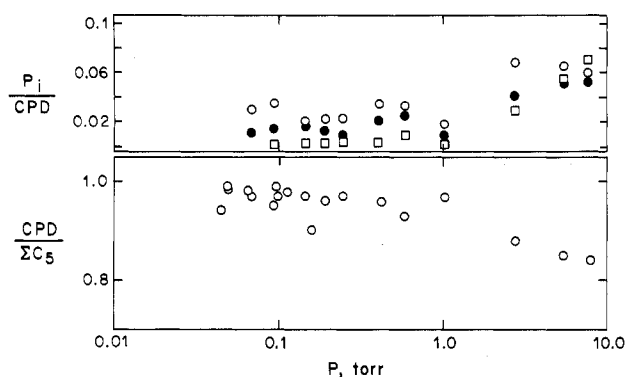


Figure 3. Top: relative yields of pentadienes and cyclopentadiene at 1029 cm^{-1} and $0.61 \text{ J/cm}^2 \leq \phi \leq 0.76 \text{ J/cm}^2$; O, *cis*-1,3-pentadiene; ●, *trans*-1,3-pentadiene; □, 1,4-pentadiene. Bottom: fractional yield of cyclopentadiene, same experimental conditions as top.

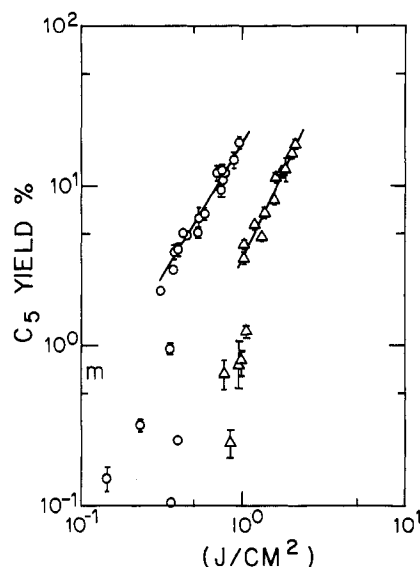


Figure 4. Dependence of yield per 10^3 pulses upon fluence at $p = 50$ mtorr. Solid line, linear least-squares fit to high fluence data: O, 1029 cm^{-1} , slope of line, 1.7; Δ, 1033 cm^{-1} , slope of line, 2.2.

measured to be 1.00 ± 0.005 . All products were identified by GC-FT/IR and GC-MS techniques. Cocondensation of product gases from multiple experiments of a high, 5–10 torr, pressure of cyclopentene with degassed acetone provided an injectable liquid sample. A small set of GC-FTIR analyses was performed on a temperature-programmed silica gel column to identify products lighter than C_5 .

Results

The infrared absorption spectrum of cyclopentene between 900 and 1100 cm^{-1} is shown in Figure 1. Cyclopentene was photolyzed at the seven indicated wavelengths distributed over two absorption bands. When the laser beam was not focused, no reaction products could be detected, even with more than 24 000 pulses and 0.62 J/cm^2 at 1048 cm^{-1} , and more than 16 000 pulses and 1.06 J/cm^2 at 1033 cm^{-1} . However, with focused radiation several reaction products were found. They were positively identified by GC/MS and GC-FTIR to be cyclopentadiene, 1,4-pentadiene, *cis*- and *trans*-1,3-pentadiene, 1,3-butadiene, propyne, ethylene, acetylene, and ethane. A trace amount of a substance that was most probably methane based on GC retention time was also seen, but the FTIR spectrum was not sufficiently resolved for positive identification. Cyclopentadiene comprised more than 95% of the reaction products under most reaction conditions except at higher pressures of cyclopentene. An adequate material balance was only obtained when hydrogen was assumed to be formed in amounts equal to

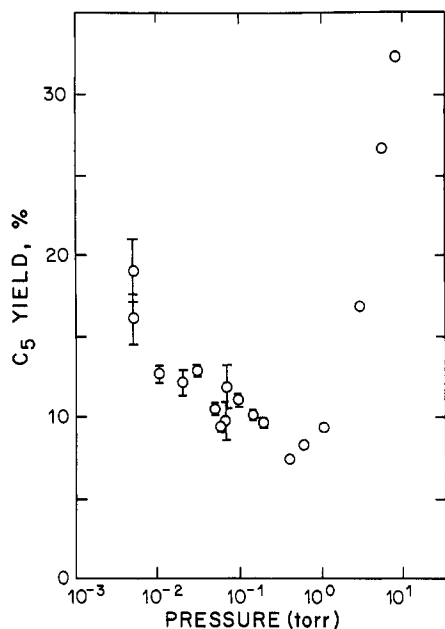


Figure 5. Dependence of C₅ yield per 10³ pulses upon cyclopentene pressure at 1029 cm⁻¹ and 0.74 J/cm².

the cyclopentadiene yield. Since the analytic techniques used were not capable of detecting hydrogen, this conclusion was not confirmed. The products having fewer than five carbons were only formed in trace amounts ($\leq 0.5\%$) and were not quantitated. In fact, they were unobservable at the lower pressures and typical conversions of 10% or less. Thus the three pentadienes accounted for virtually all of the minor products observed.

A few experiments were done with 1-methyl-1-cyclopentene at 1029 and 1019 cm⁻¹, on the blue side of an absorption band with $\tilde{\nu}_{\max} \sim 1000$ cm⁻¹. Figure 2 shows the relevant portion of the IR spectrum. Analysis of reaction products by GC-FTIR permitted tentative identification of trace amounts of propyne and 2-methyl-1,3-butadiene, as well as positive identification of a small amount of cyclopentadiene (~ 3 –7%). Two GC peaks suspected of being methylcyclopentadienes were found, but unfortunately positive identification was not possible because published IR spectra for these species could not be found. The spectra did not correspond with published spectra for any of the methyl-pentadienes. Spectra were qualitatively consistent with the molecular structure of methylcyclopentadiene, which is the major product of the methylcyclopentene thermal decomposition.⁶ The GC retention time is also consistent with this assignment. We tentatively conclude that the major products from IRMPD of methylcyclopentene are methylcyclopentadiene and, by inference, hydrogen.

In cyclopentene photolysis no dependence of the composition of C₅ products on fluence or extent of reaction could be established. Experiments carried out to greater than 90% conversion at 1033 cm⁻¹ gave pentadiene to cyclopentadiene ratios that were not significantly different from values found at the smallest conversions (<5%). However, some changes of C₅ product distribution with wavelength and pressure were found. The C₅ product distributions at 1048, 1040, 1033, and 1029 cm⁻¹ were comparable provided the pressures were similar. See Figure 3 for the distribution of C₅ products. No pentadienes or fragmentation products were observed at either 977 or 965 cm⁻¹, because at the low pressure (50 mtorr) and low conversions (0.23% and 0.13% for 2500 pulses) there was insufficient detection sensitivity for minor products. However, at 1061 cm⁻¹, the pentadienes were not detected even at 13.5% conversion, there they would have been observable if formed in amounts comparable to the 1048–1029-cm⁻¹ interval. It is clear from Figure 3 that all three pentadienes increase at the expense of cyclopentadiene as pressure increases and, furthermore,

(6) N. Turner, *J. Am. Chem. Soc.*, **91**, 7678 (1969).

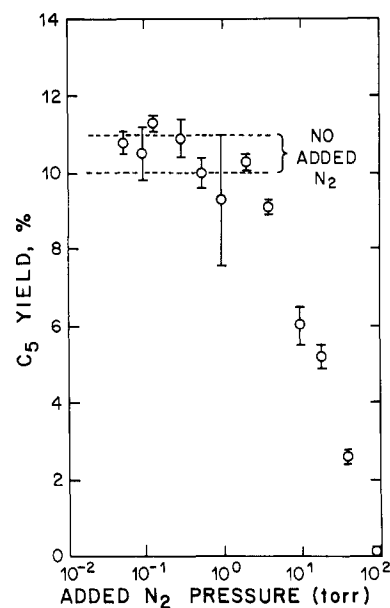


Figure 6. Dependence of C₅ yield per 10³ pulses upon pressure of added N₂ at 1029 cm⁻¹ and 0.74 J/cm². Cyclopentene pressure, 54 mtorr. Bracket indicates range of C₅ yield without N₂, and 50 mtorr $\leq P_{\text{cyclopentene}} \leq 200$ mtorr for comparison.

that *trans*-1,3-pentadiene, which is the least product at low pressures, grows to be the greatest at high pressure. A series of experiments done at 1029 cm⁻¹ with fluences about 0.72 J/cm², cyclopentene pressure of 54 mtorr, and increasing dilution by N₂, up to 98 mmHg, showed 1,4-pentadiene and *cis*-1,3-pentadiene yields relative to cyclopentadiene that were constant and similar to low pressure experiments without N₂ added. However, no *trans*-1,3-pentadiene could be detected in these experiments.

In contrast to the C₅ product distribution, the total yield of C₅ products shows strong dependence upon wavelength, fluence, and pressure. The relationship between yield of C₅ products per 10³ pulses and fluence at 1033 and 1029 cm⁻¹ is given in Figure 4. The C₅ yield is calculated as the sum of pentadienes plus cyclopentadiene divided by that total plus unreacted cyclopentene. Laser fluence of the unfocused beam ranged from 0.2 to 1 J/cm². Erratic laser behavior at low pulse energies made it necessary to attenuate the beam to achieve reliable results at fluences less than 0.3 J/cm². This was accomplished with either clouded NaCl flats or polyethylene sheets. The lines drawn at higher fluences represent slopes found by linear least-squares fitting the data.

Figure 5 shows C₅ yield per 1000 pulses at 1029 cm⁻¹ for cyclopentene pressure between 1 mtorr and 10 torr. In this plot the data were corrected to a fluence of 0.74 J/cm² with the relationship

$$Y_{0.74} = Y_{\phi}(0.74/\phi)^{1.7} \quad (1)$$

where Y_{ϕ} is yield at fluence ϕ , $Y_{0.74}$ is yield at a fluence of 0.74 J/cm², and 1.7 is the slope of the high fluence data at 1029 cm⁻¹ from Figure 4. Figure 6 shows the effect of added N₂, up to 100 torr, on the C₅ yield per 1000 pulses at 1029 cm⁻¹ and fluences corrected to 0.74 J/cm² as above. In this series of experiments the cyclopentene pressure was held constant at 54 mtorr.

Table I gives the C₅ yields per 10³ pulses from cyclopentene at the seven wavelengths indicated in Figure 1, and the single wavelength for methylcyclopentene. All of the yields are at a fluence of 0.6 J/cm², either taken directly from experimental data, or corrected from the log yield vs. log fluence plots, and are in the lower pressure range where yields are independent of pressure. These data are also plotted in Figure 1.

When N₂ was omitted from the laser gas mixture the laser output waveform consisted of only the sharp initial peak having a width of ~ 150 ns, whereas with N₂ present a second, broad peak having a width of ~ 2 μ s was present. A pair of experiments done

TABLE I: Wavelength Dependence of Product Yields

wavenumber, cm ⁻¹	absorbance, ^a %	C ₅ yield per 10 ³ pulses, ^b %
1061	8.5	1.0
1048	16.6	0.2
1040	9.3	3.3
1033	9.9	4.8
1029	9.7	8.0
977	6.5	<0.1
965	6.3	<0.1
1019	9.4	>16 ^c

^a Absorbance of 10.7 torr of cyclopentene in an 8.0-cm absorption path. ^b At 0.6 J/cm² and pressures below ~0.5 torr.

^c Approximate C₆ yield from 1-methylcyclopentene at 0.6 J/cm².

with and without added N₂, but at the same fluence (0.43 J/cm²), gave identical C₅ yields of 5–2% at 1029 cm⁻¹, showing that laser intensity effects were unobservable.

Discussion

The thermal decomposition of cyclopentene is a homogeneous, unimolecular reaction^{1a} which occurs by intramolecular elimination of molecular hydrogen to yield cyclopentadiene. Baldwin⁷ showed that at 550 °C the symmetry allowed⁸ 3,5 elimination is the dominant path although some "disallowed" 3,4 elimination occurs. At 1100–1300 K, however, the 3,4 elimination is of about equal importance with 3,5 elimination.⁹ Knecht^{1c} showed that formation of the secondary products ethylene and propylene, which can be explained by a reaction sequence initiated by addition of atomic hydrogen cyclopentene, increases in importance with increasing conversion. Increasing influence of secondary reactions in the later stages of the reaction may also be reflected in the decreasing unimolecular rate coefficients as measured by the pressure increase.^{1a,b} Lewis et al.¹⁰ noted that the yield of fragmentation products increased with increasing temperature in their shock tube work.

The infrared multiple-photon decomposition of cyclopentene is similar to the thermal decomposition in the sense that cyclopentadiene is also the principal product. Furthermore, all of the C₁–C₄ products found in the laser-induced reaction have previously been reported in thermal studies, although two products that were found in pyrolysis, allene^{1c,10} and cyclopentane,^{1a,11} were not found here. There are also some differences in the products obtained from these two methods of driving the reaction. The pentadienes found in this study have not been reported in the published literature on cyclopentene pyrolysis, although evidence for 1,4-pentadiene has recently been found in shock tube work.¹² Also, the C₁–C₄ species formed in trace amounts in the laser-induced reaction are produced in yields up to a few percent in pyrolysis.

A possible mechanism for the formation of pentadienes from cyclopentene would be C–C bond breaking and intramolecular 1,2 and 1,4 H shifts. Since experiments to test this hypothesis were not done, it remains speculative although not unlikely. The activation energy for such a process is expected to be greater than the 60 ± 1 kcal/mol activation energy for H₂ elimination,¹ suggesting that infrared laser excitation is capable of exciting cyclopentene to higher energies than are attained in conventional pyrolysis. The detection of 1,4-pentadiene in shock tube experiments in the vicinity of 1200 K,¹² but not at lower temperatures, might be explained thusly. Pentadiene formation via higher energy channels than required for cyclopentadiene should be revealed by observations of enhanced pentadiene yields at higher fluences. We were unable to establish whether this was the case because at low

fluences yields were low and pentadienes could not be reliably determined. Accurate pentadiene yields were thus obtained over only a limited range of fluence. In connection with the above, it is interesting to note that Teng, Weitz, and Lewis¹³ found that multiple-photon infrared-induced reaction of *cis*- or *trans*-1,3-pentadiene resulted in quantitative conversion to cyclopentadiene plus hydrogen. Failure to observe either *cis*- or *trans*-1,3-pentadiene in any of the thermal work may be due to rapid addition to cyclopentadiene. The Arrhenius expression for this reaction has been reported to be $k(T) = 2.2 \times 10^{13} \exp(-34000/RT)$ L mol⁻¹ s⁻¹.¹⁴

High yields of the C₃ products could be obtained at low pressure (~0.05 torr) where thermal effects must be virtually absent, so gas temperatures remain nearly constant. The largest yield, 92%, was obtained for 15 × 10⁴ pulses at 1033 cm⁻¹, 0.011 torr, and 0.68 J/cm². Larger yields could have been obtained at higher fluences and longer irradiation times. Since the dehydrogenation of cyclopentene is endothermic by 24.5 kcal/mol, the 298 K thermal equilibrium yield is about 10⁻⁴, even at low pressure. The results clearly show that reaction yields which are orders of magnitude larger than thermal equilibrium yields are attainable by the laser-induced reaction.

Two normal coordinate analyses of cyclopentene have appeared in the literature.^{2,3} There is agreement that the absorption feature between 1000 and 1100 cm⁻¹ shown in Figure 1 contains the PQR branches of a CH₂ motion in the position α to the double bond. This motion was described by Sverdlov and Krainov² as a CH₂ rock and by Villarreal et al.³ as an in-phase CH₂ twist. The latter reported considerable frequency mixing, as predicted by Harris and Longshore,¹⁵ between skeletal modes and carbon–hydrogen bending fundamentals. Excitation in this band promotes a motion that may be similar to the reaction coordinate for 3,5 H₂ elimination. The band between 950 and 1000 cm⁻¹ is probably a C–C stretch or a skeletal deformation.¹⁵ The low product yields obtained from cyclopentene excitation in this band, compared with the 1048-cm⁻¹ band, may be attributable to the difference in absorption cross section of the fundamentals rather than any advantage in pumping the CH₂ twist over pumping ring frequencies. One would not expect any vibrational mode selectivity unless intramolecular vibrational energy relaxation were slow compared with the reaction rate. Intramolecular vibrational energy redistribution in highly vibrationally excited polyatomic molecules has usually been found to occur in a few picoseconds.

It is interesting to note that excitation at 1048 cm⁻¹, which coincides with the position of the Q branch absorption maximum, results in a very low yield (see Figure 1) in spite of the large absorption coefficient. Excitation at 1061 cm⁻¹ in the R branch gives a larger yield, and in the P branch yields are larger yet, showing a red shift.

As indicated above, changes in yield with laser pulse length could not be detected for pulses of identical total energy. It has been pointed out that the separation of fluence and intensity effects requires carefully defined beam geometry and pulse shape,¹⁶ and proper characterization was not possible in this work. However, lacking any evidence to the contrary, fluence will be used rather than intensity in the following. This should cause no difficulty since nearly all of the work was done at constant pulse length.

Reasonable yields could only be obtained by focusing the laser beam to fluences at the beam waist estimated to be upward of 100 J/cm². The largest low-pressure conversions attained were in the vicinity of 10–20% per 1000 pulses at 1029 cm⁻¹. This may be contrasted with work on the infrared multiple-photon isomerization of vinylcyclopropane,¹⁷ an isomer of cyclopentene.

(13) P. P. Teng, E. Weitz, and F. D. Lewis, *J. Am. Chem. Soc.*, **104**, 5518 (1982).

(14) V. P. Bulychev, K. P. Lavorskii, and A. N. Rumyantsev, *Neftikhi-miya*, **6**, 690 (1966).

(15) W. C. Harris and C. T. Longshore, *J. Mol. Struct.*, **16**, 187 (1973).

(16) M. N. R. Ashfold, C. G. Atkins, and G. Hancock, *Chem. Phys. Lett.*, **80**, 1 (1981).

(17) W. E. Farneth, M. W. Thomsen, N. L. Schultz, and M. A. Davies, *J. Am. Chem. Soc.*, **103**, 4001 (1981).

(7) J. E. Baldwin, *Tetrahedron Lett.*, 2953 (1966).

(8) R. B. Woodward and R. Hoffman, "The Conservation of Orbital Symmetry", Verlag Chemie, Berlin, 1970, pp 143–4.

(9) D. K. Lewis, M. A. Greaney, and E. L. Sibert III, *J. Phys. Chem.*, **85**, 1783 (1981).

(10) D. K. Lewis, M. Sarr, and M. Keil, *J. Phys. Chem.*, **78**, 436 (1974).

(11) C. J. Grant and R. Walsh, *Chem. Commun.*, 667 (1969).

(12) D. K. Lewis, private communication.

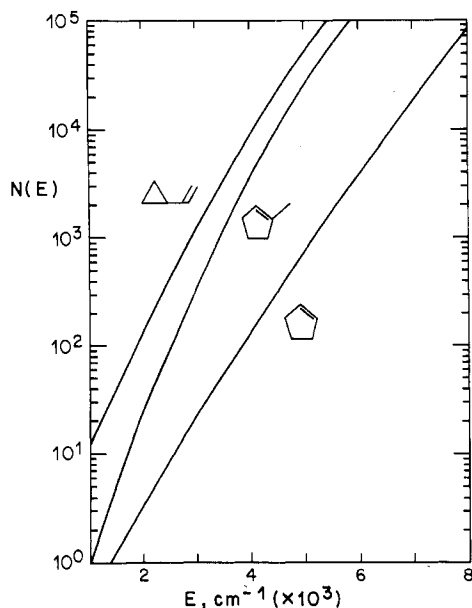


Figure 7. Vibrational state densities for vinylcyclopropane, cyclopentene, and 1-methylcyclopentene. See Appendix for details.

Unfocused radiation with fluences of 2–3 J/cm² gave more than 20% conversion with only 200 pulses at 933 cm⁻¹. Vinylcyclopropane may be easier to drive because the activation energy for the lowest reaction channel, to give cyclopentene, is only 49.7 kcal/mol,¹⁸ compared with 60 kcal/mol for cyclopentene dehydrogenation. However, the activation energy for 1,4-pentadiene production from vinylcyclopropane, 57.3 kcal/mol,¹⁸ is only slightly less than the 59–61 kcal/mol required for cyclopentene, and 9% of 1,4-pentadiene was reported in IRMPD of vinylcyclopropane¹⁷ at fluences where we observe no reaction of cyclopentene. This suggests that energetic considerations alone cannot explain the observed differences. The infrared multiple-photon trans to cis isomerization of 1,3-pentadiene¹³ also occurs more readily than does dehydrogenation of cyclopentene, although in this case it may be the lower energy barrier for isomerization (53 kcal/mol) that is responsible.

If cyclopentene were tightly bottlenecked due to rotational hole burning, we might expect yields to increase with increasing pressure in the lower pressure regime where rotational relaxation, but no significant vibrational relaxation, occurs during the laser pulse. No evidence of this was found with added N₂ (Figure 6) or neat cyclopentene (Figure 5).

Figure 7 compares exact count¹⁹ harmonic oscillator vibrational state densities for cyclopentene and vinylcyclopropane. It is evident that the onset of the quasicontinuum must occur earlier in vinylcyclopropane than in cyclopentene, and this may provide at least part of the explanation of the observed differences. The higher vibrational state density of vinylcyclopropane which occurs in spite of low-lying frequencies for some of the ring modes for cyclopentene, including a ring puckering at 127 cm⁻¹,³ can be attributed to its internal rotor. The Appendix gives the harmonic oscillator frequencies used.

The experiments with 1-methylcyclopentene were done to see if this molecule would react more easily than cyclopentene. Thermal decomposition of methylcyclopentene has been reported to occur by unimolecular loss of molecular hydrogen with an activation energy 2.3 kcal/mol higher than cyclopentene.⁶ Infrared spectra of methylcyclopentene and cyclopentene show that at 1019 cm⁻¹ the absorption cross sections are very nearly identical (absorbance of methyl cyclopentene, 9.4%, cyclopentene 9.7%, each at 10.65 torr) so that laser excitation rates would be nearly equal for the first photon at equal pressure and fluence. The yields from

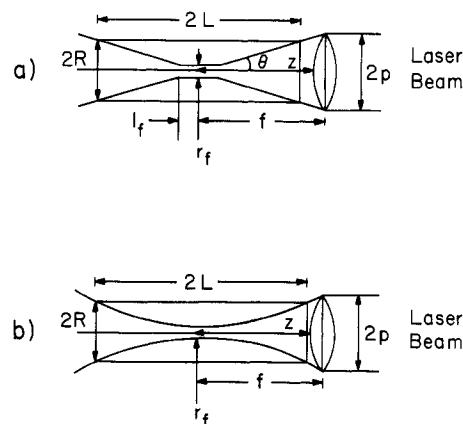


Figure 8. (a) Idealization of focused beam geometry, from Speiser and Jortner.²⁴ (b) Hyperboloid beam waist used in present model.

methylcyclopentene are greater by at least a factor of 2 at 0.6 J/cm², and at 0.26 J/cm² they are greater by about a factor of 20. The methylcyclopentene excitation wavelength is blue shifted from the peak absorbance. If a red-shift improvement for conversion of methylcyclopentene comparable to that found for cyclopentene were to occur, the yield enhancement for methylcyclopentene over cyclopentene might be expected to be ~20 at 0.6 J/cm² and ~200 at 0.26 J/cm². The above are significant differences which occur in spite of a higher energy requirement for methylcyclopentene. They can be attributed to increases in vibrational state density due to the methyl group, see Figure 7.

The fluence dependence of the yield shown in Figure 4 as a double logarithmic plot is typical of many multiple-photon infrared reactions. The steep initial rise at low yields may be interpreted as due to a power law for a high-order multiphoton process, given by

$$Y \sim \phi^n \quad (2)$$

where ϕ is laser fluence and n is the order of the multiphoton process. An alternative explanation of the steep initial rise of such plots in terms of a non-steady-state effect has been pointed out by Quack.²⁰

At higher fluences, the dependence of cyclopentene yield on fluence is less pronounced. It has been shown that, in experiments with focused beams, experimentally observed yield-fluence relationships given by $Y \sim \phi^{3/2}$ at high fluences could be explained as a consequence of expansion of the saturated interactive volume out of the beam waist into the diverging conical section with increasing laser energy.^{21,22} These models predict that the geometrical effect obscures any information on the true intensity dependence of the multiple-photon process. A linear least-squares fit to the high laser energy data of Figure 4 gives slopes of 1.7 at 1029 cm⁻¹ and 2.2 at 1033 cm⁻¹. The former is close to the value of 1.5 from model predictions, but the latter is significantly greater, and we conclude that the models fail to give a satisfactory account of the cyclopentene high-energy yield-fluence data. In the following, we present a simple phenomenological model that is capable of accounting qualitatively for our observations.

Lyman et al.²³ approximated the focused beam geometry by two coaxial cones with touching apexes, and concluded that the maximum observable dependence on laser intensity would be $I^{3/2}$. Speiser and Jortner²⁴ idealized the beam waist as a right cylinder, attached to diverging truncated cones, Figure 8. If we use the concept of a saturation threshold and assume eq 2 holds, the model predicts that, at intensities below the saturation threshold, $Y \sim$

(20) M. Quack, *Ber. Bunsenges. Phys. Chem.*, **82**, 1252 (1978).

(21) I. N. Arutyunyan, G. A. Askar'yan, and V. A. Pogoyan, *Sov. Phys. JETP*, **31**, 548 (1970).

(22) S. Speiser and S. Kimel, *Chem. Phys. Lett.*, **7**, 19 (1970).

(23) J. Lyman, S. D. Rockwood, and S. M. Freund, *J. Chem. Phys.*, **67**, 4545 (1977).

(24) S. Speiser and J. Jortner, *Chem. Phys. Lett.*, **44**, 399 (1976).

(18) C. A. Wellington, *J. Phys. Chem.*, **66**, 1671 (1962).

(19) S. E. Stein and B. S. Rabinovitch, *J. Chem. Phys.*, **58**, 2438 (1973).

I^n , whereas at intensities greater than threshold, $Y \sim I^{3/2}$ with a discontinuity in slope at the saturation threshold.

It is well-known that when a single-mode strictly Gaussian beam is focused the axial geometry obtained is a hyperbola.²⁵ Two reports describing results of model calculations of MPD yields for focused beams with a hyperbolic beam waist have recently appeared.^{26,27} Our independent analysis follows Speiser and Jortner,²⁴ but substitutes a circular hyperboloid of revolution, Figure 8b, for the "dog bone" approximation to describe beam waist geometry.

The photoreaction probability per pulse in a laser field of amplitude E is assumed to follow a simple power law relationship given in reduced form by

$$\Gamma(E) = \alpha(E/E_c)^k \quad E < E_c$$

$$= \alpha \quad E \geq E_c$$

where $k = 2n$ (the exponent is not necessarily associated with the order of a multiphoton process²⁰, E_c is the critical amplitude providing for the onset of saturation effects, and $\alpha \leq 1$ is a dimensionless parameter determined by the laser pulse characteristics. For an optically thin sample $E(z)r(z) = \text{constant}$. In the case of a circular hyperboloid, $(r^2/a^2) - (z^2/c^2) = 1$, it is seen that $r(z) = (a^2 + a^2z^2/c^2)^{1/2}$ so that we can write

$$E(z) = \frac{E_f r_f}{r(z)} = \frac{E_f c}{(c^2 + z^2)^{1/2}} \quad (3)$$

since $r_f = a$, the radius at the beam waist minimum. The parameter c is related to the eccentricity of the hyperbola by $e = (a^2 + c^2)^{1/2}/a$. The slopes of the asymptotes of the hyperbola are also related to c , being $\pm a/c$. In general, for a sharper focus c will get smaller. We can also write $\Gamma(E) = \Gamma(E(z)) = \Gamma(z)$ if we assume that the beam has a uniform radial intensity profile.

To establish correspondence to experimentally observable parameters consider an initially uniform sample with concentration n_0 . After a laser pulse, the reaction product concentration n_1^P is given by $n_1^P(z) = \Gamma(z)n_0$ and the total product yield is obtained via integration over the cell

$$\langle n_1^P \rangle = \int_V n_1^P(z) dV = n_0 V \langle \Gamma \rangle$$

where

$$\langle \Gamma \rangle = V^{-1} \int_V \Gamma(z) dV$$

is the experimental photoreaction probability per pulse. It is seen at once that this model ignores axial and radial mixing due to diffusion and other means. Exclusion of gross mixing due to natural convection from heated gases appears to be justified,²⁸⁻³⁰ and diffusion will take place more slowly than the timescale of the chemistry in a single pulse. The form of $\Gamma(E)$ gives us the possibility of three regimes. The amplitude at the focus, E_f , may be less than E_c or greater than or equal to E_c . In the latter case the critical threshold will be crossed at z_c and z_c may be $0 \leq z_c \leq L$ or $z_c > L$. We will not consider the case $z_c > L$ and so have two cases:

$$E_f < E_c \quad z_c \text{ does not exist}$$

$$E_f \leq E_c \quad 0 \leq z_c \leq L$$

Using eq 3 see that

$$z_c = [(E_f/E_c)^2 - 1]^{1/2}c$$

consider first the case $E_f < E_c$, or $\Gamma(E) = \alpha(E(z)/E_c)^k$.

$$\langle \Gamma \rangle = V^{-1} \int_V \alpha(E(z)/E_c)^k dV$$

or

$$= 2V^{-1}\alpha\pi(E_f c/E_c)^k(a/c)^2 \int_0^L (c^2 + z^2)^{(2-k)/2} dz \quad (4)$$

Consider now the case $E_f \geq E_c$, with two regions: I, $0 \leq z \leq z_c$, and II, $z_c < z \leq L$. In region I $\Gamma(E) = \alpha$ and

$$\langle \Gamma \rangle = 2V^{-1}\alpha\pi(a/c)^2 \int_0^{z_c} (c^2 + z^2) dz \quad (5)$$

In region II $\Gamma(E) = \alpha(E(z)/E_c)^k$, so

$$\langle \Gamma \rangle = 2V^{-1}\alpha\pi(E_f c/E_c)^k(a/c)^2 \int_{z_c}^L (c^2 + z^2)^{(2-k)/2} dz \quad (6)$$

Combining (5) and (6) we have

$$\langle \Gamma \rangle = 2\pi\alpha V^{-1}(a/c)^2 \left[\int_0^{z_c} (c^2 + z^2) dz + (E_f c/E_c)^k \int_{z_c}^L (c^2 + z^2)^{1-n} dz \right] \quad (7)$$

The laser intensity, I , is related to the amplitude by $I \propto E^2$. To remain general, we are interested in the reduced intensity

$$X = I/I_c = (E(z)/E_c)^2 \quad (8)$$

Rewriting eq 4 and 7 in terms of X , and lumping all common constants into the factor A , we find for X at the focus

case 1: $X < 1$

$$\langle \Gamma \rangle = AC^{2n} X^n \int_0^L (c^2 + z^2)^{1-n} dz \quad (9)$$

case 2: $X \geq 1$

$$\langle \Gamma \rangle = A \left[\frac{C^3}{3} (X-1)^{1/2} (X+2) + X^n C^{2n} \int_{C(X-1)^{1/2}}^L (c^2 + z^2)^{1-n} dz \right] \quad (10)$$

$$A = 2\pi\alpha V^{-1}(a/c)^2$$

The value of $\langle \Gamma \rangle$ is related directly to the yield, being the average probability of reaction per pulse. Equation 9 shows that the order of the process, n , is revealed in case 1. The first term in eq 10 gives rise to the 3/2 power law for large X , while the second term contributes a varying amount dependent on the values of X and n . For $X \geq 1$, however, the function is smooth rather than discontinuous at $X = 1$. This must be because smooth rather than discontinuous geometry is used in the model, rather than other model deficiencies, such as the simple form of $\Gamma(E)$. Figure 9 is $\log \langle \Gamma \rangle / A$ vs. $\log X$ plot of numerical calculations obtained by using actual beam geometry parameters measured for a beam passing through a 40-cm f.l. lens used in experiments described below. The slope decreases smoothly from a limiting value of n in the low fluence regime toward a limiting value of 3/2 in the high fluence regime. The present numerical calculations reveal that the slope reaches a minimum value slightly less than 3/2 before reaching the limit of 3/2 at large X . This is not readily apparent from Figure 4 because of the limited range of X plotted.

The focused laser beam in this work was a reasonably good geometrical approximation to the model beam used in making calculations. The radial intensity profile varied by only about 20% across the 2-cm² circular aperture used to define the beam before focusing. This was determined from superposition of the aperture onto a power contour map of the entire beam made by placing

(25) A. Yariv, "Introduction to Optical Electronics", 2nd ed, Holt, Rinehart and Winston, New York, 1976.

(26) I. Hanazaki, *Appl. Phys. B*, **26**, 111 (1981).

(27) K. Takeuchi, I. Inoue, R. Nakane, Y. Makide, S. Kaot, and T. Tomimaga, *J. Chem. Phys.*, **76**, 398 (1982).

(28) R. N. Zitter, D. F. Koster, A. Cantoni, and J. Pleil, *Chem. Phys.*, **46**, 107 (1980).

(29) S. W. Bodman, P. L. T. Brian, and T. C. Change, *AIChE J.*, 1304 (1971).

(30) H. S. Carslaw and J. C. Jaeger, "Conduction of Heat in Solids", 2nd ed, Oxford University Press, London, 1959.

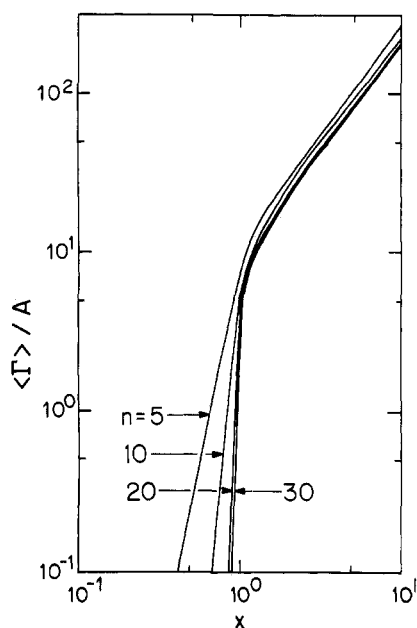


Figure 9. Calculations of dependence of reaction probability on reduced fluence or reduced intensity, calculated from eq 9 and 10.

a 0.4-cm-diameter aperture in front of the power meter, and scanning the meter horizontally and vertically through the unfocused beam at intervals. The axial profile of the focused beam was measured from prints made on thermal paper for positions away from the beam waist. This procedure was not satisfactory near the focus since the multimode structure of the beam produces complex spot patterns. The radius at $z = 0$ was found to be 0.05 cm by measuring the power transmitted through an 0.008-in.-diameter aperture that was scanned across the beam by a micrometer driven translation stage. This fixed the value of a in the equation $(r^2/a^2) - (z^2/c^2) = 1$. Then values of c calculated at $z = 20$ cm and $z = 40$ cm, where thermal prints gave good values of r , resulted in $c = 2.52$ and 2.58 , respectively. The close agreement in these values gave assurance that the focused laser beam was a good approximation to a hyperbola, and that comparisons between experimental results and model predictions may be justified.

Since the data displayed in Figure 4 were all obtained at the same laser pulse length, fluence may be used interchangeably with intensity in making comparisons of model predictions with experiment. The yields at low fluence have considerable scatter due to the small amounts of material analyzed, and a value of n cannot be reliably established. The higher fluence data are not of sufficient quality to unambiguously reveal the curvature predicted by the model. However, linear least-squares analysis gives slopes significantly greater than $3/2$, which we take to be indicative of a transition region heading toward a limiting slope of $3/2$ at higher fluences. It was not possible to test this by further increasing the fluence. Nevertheless, we conclude that the data are consistent with model predictions. Furthermore, it is not necessary for the yield of multiphoton processes in focussed laser beams to only follow either fluence to the $3/2$ power or the n th power; observations of curvature or of apparent intermediate dependences may be expected between these limits.

While observations of the $3/2$ power relationship have been reported, for example, in SF_6 ,^{31,32} there is also evidence of the behavior described above. Fluorescence from SiF produced in the CO_2 laser-induced dissociation of SiF_4 approaches a $3/2$ power law for high laser power.³³ Logarithmic plots of yield vs. fluence

frequently give slopes greater than $3/2$, and less than the minimum number of photons required for reaction. The multiphoton decomposition of ethylene provides a good example of linear low fluence region followed by curvature toward a limiting slope of $3/2$.³⁴ Other examples of qualitatively similar plots may be found.^{27,35,36}

The dependence of C_5 yield on the initial pressure of neat cyclopentene is similar in form to the pressure results reported by others in both low- (less than ~ 1 torr)³⁷⁻⁴¹ and high-pressure ranges.^{38,40,42,43} Figure 5 shows yields decreasing to a minimum in the vicinity of 0.5 torr and increasing thereafter. In the low-pressure region the falloff is probably due to collisional deactivation. As the pressure increases from 0.001 to 1 torr the collisionless time (based on gas kinetic collisions with a hard-sphere diameter for cyclopentene of 8×10^{-8} cm) decreases from 72 to 0.072 μs . The fact that a three magnitude increase in the rate of collisions produces only a factor of about 4 decrease in yield must mean either that reaction is essentially complete during the pulse length or that deactivation is extremely inefficient. The former seems more probable.

The rise in yield at higher pressures may be due to pyrolysis from bulk heating. At higher gas densities the number of molecules interacting with the laser radiation increases, as does the rate of collisional energy dissipation. However, diffusional loss of hot molecules from the irradiated volume to cold surroundings decreases. The result may be a thermal, or nearly thermal, reaction with high yields due to the higher energy deposition at higher pressures. Increased yields might also be attributable to energy pooling,⁴⁴ or to removal of bottlenecks. The results with added N_2 suggest that collisional removal of bottlenecks is not important, since yields continue to decrease to a pressure of 200 torr.

Experiments in which the neat cyclopentene pressure was held constant at about 0.054 torr, the fluence at about 0.72 J/cm^2 , and N_2 buffer gas was added in varying amounts are shown in Figure 6 as C_5 yield plotted against added N_2 pressure. The critical feature is that the yield does not differ, within experimental error, from the neat cyclopentene experimental result until the pressure of added N_2 gas gets above roughly 3 torr. This supports the suggestion made earlier that most of the reaction occurs within the laser pulse width. The N_2 collisions do not seriously inhibit the reaction through deactivation until above 3 torr. This is not unexpected since cyclopentene is a more efficient collider than nitrogen.

Acknowledgment. The assistance of the National Science Foundation, Grant No. ENG-7911586, in purchasing the TEA CO_2 laser is gratefully acknowledged. Support of the experimental program was from the National Science Foundation under Grant No. CPE-8023180. Vibrational state densities were computed by M. Yerram.

(34) N. C. Peterson, R. G. Manning, and W. Braun, *J. Res. Nat. Bur. Stand. U.S.A.*, **83**, 117 (1978).

(35) D. S. King and J. S. Stephenson, *J. Am. Chem. Soc.*, **100**, 7151 (1978).

(36) S. V. Filseth, J. Danon, D. Feldmann, J. D. Campbell, and K. H. Welge, *Chem. Phys. Lett.*, **63**, 615 (1979).

(37) S. Koda, Y. Ohnuma, T. Onkawa, and S. Tsuchiya, *Bull. Chem. Soc. Jpn.*, **53**, 3447 (1980).

(38) H. L. Dai, A. H. Kung, and C. B. Moore, *J. Chem. Phys.*, **73**, 12 (1980).

(39) W. Braun and J. R. McNealy, *J. Phys. Chem.*, **84**, 2521 (1980).

(40) J. M. Preses, R. E. Weston, and G. W. Flynn, *Chem. Phys. Lett.*, **46**, 69 (1977).

(41) W. Braun, J. T. Herron, W. Tsang, and K. Churney, *Chem. Phys. Lett.*, **59**, 492 (1978).

(42) M. H. Back and R. A. Back, *Can. J. Chem.*, **57**, 1511 (1979).

(43) P. A. Hackett, C. Willis, M. Brown, and E. Weinberg, *J. Phys. Chem.*, **84**, 1873 (1980).

(44) I. Oref, *J. Chem. Phys.*, **75**, 131 (1981).

(45) J. R. Durig, A. C. Shing, W. E. Bucy, and C. J. Wurrey, *Spectrochim. Acta, Part A*, **34**, 525 (1978).

(31) G. Hancock, J. D. Campbell, and K. H. Welge, *Opt. Commun.*, **16**, 177 (1976).

(32) T. P. Cotter and W. Fuss, *Opt. Commun.*, **16**, 177 (1976).

(33) N. R. Isenor, V. Merchant, and R. S. Hallworth, *Can. J. Phys.*, **51**, 1281 (1973).

Appendix

Vibrational state densities for cyclopentene, 1-methylcyclopentene, and vinylcyclopropane were computed from harmonic oscillator models by exact count.¹⁹ Fundamental vibrational wavenumbers used were: cyclopentene,³ 3070, 3068, 2963, 2938, 2933, 2903, 2882, 2860, 1617, 1473, 1448, 1438, 1353, 1302, 1268, 1209, 1207, 1134, 1128, 1109, 1047(2), 1037, 962, 933, 896, 879, 695(2), 600, 593, 390, 127; 1-methylcyclopentene,⁴⁵ 3052, 2966, 2960, 2955, 2936, 2924, 2903, 2868, 2863, 2858, 1662, 1474, 1456, 1446, 1436, 1383, 1335, 1299, 1261, 1218, 1203, 1149, 1135, 1064,

1032, 1009, 1006, 928, 906, 888, 879, 873, 858, 817, 788, 642, 574, 432, 330, 228, 170, 104; vinylcyclopropane,¹⁷ 3050 (8), 1625, 1425 (3), 1300 (20), 1050 (2), 1000 (8), 900, 800 (2), 425, 310 (2), 50. In methylcyclopropane and vinylcyclopropane the methyl and vinyl groups were treated as torsional vibrations of 170 and 50 cm⁻¹, respectively.

Registry No. Cyclopentene, 142-29-0; cyclopentadiene, 542-92-7; 1,4-pentadiene, 591-93-5; *cis*-1,3-pentadiene, 1574-41-0; *trans*-1,3-pentadiene, 2004-70-8; 1-methylcyclopentene, 693-89-0; vinylcyclopropane, 693-86-7.

Electronic Spectra from Molecular Dynamics: A Simple Approach

John P. Bergsma, Peter H. Berens, Kent R. Wilson,*

Department of Chemistry, University of California, San Diego, La Jolla, California 92093

Donald R. Fredkin,

Department of Physics, University of California, San Diego, La Jolla, California 92093

and Eric J. Heller

Theoretical Division, T-12, Los Alamos National Laboratory, Los Alamos, New Mexico 87545

(Received: August 12, 1983)

A method is illustrated for computing the contours of electronic absorption bands from classical equilibrium or nonequilibrium molecular dynamics (or equally for equilibrium systems from Monte Carlo or explicit integration over coordinates). The inputs to the calculations are the potential energy curves for the different electronic states and the electronic transition dipole moments between the states as functions of nuclear coordinates. A simple quantum correction by temperature scaling is demonstrated for the thermal equilibrium case. A test is carried out for the I₂ visible absorption spectrum involving transitions from the ground X 0_g⁺(¹Σ) to the excited A 1_u(³Π), B 0_u⁺(³Π) and B' 1_u(¹Π) states, for thermal equilibrium gas-phase I₂. The electronic band contours are computed and shown to be remarkably similar to the measured contours. This method and others such as the methods of Lax, Lee, Tellinghuisen, and Moeller and the Landau-Zener-Stuckleberg-Tully-Preston surface hopping approach are shown all to be mutually equivalent, while the usual reflection method is shown to be related but nonequivalent.

I. Introduction

In this paper we show how molecular dynamics can be used in a simple manner to compute the contours of electronic absorption bands. The motivation for this work is to compute transient electronic spectra for many atom systems.^{1,2} We could equally use Monte Carlo or explicit integration over coordinates to compute equilibrium electronic absorption bands. However, molecular dynamics provides the only means to calculate these band contours in a nonequilibrium system. Thus, by demonstrating that molecular dynamics yields the correct absorption band contour

for the equilibrium case, we can justify using this technique in the nonequilibrium case. We have already elsewhere^{1,2} applied the methods derived in this paper to the calculation of the transient electronic absorption spectra from a chemical reaction occurring in solution. In another paper³ the electronic absorption spectrum for an initially thermal equilibrium system is computed by a time-dependent wave packet technique, and the result for the same I₂ molecular test case can be compared to the more classical technique developed here.

In section II we discuss the theory which we will use, as well as a harmonic quantum correction appropriate for thermal equilibrium. Section III contains a comparison with other semiclassical approaches for electronic spectra. The potential energy and electronic transition dipole vs. internuclear distance functions used to compute the sample I₂ visible absorption band contours are presented in section IV. Section V discusses the computational

(1) P. Bado, P. H. Berens, J. P. Bergsma, S. B. Wilson, K. R. Wilson, and E. J. Heller in "Picosecond Phenomena", Vol. III, K. B. Eisenthal, R. M. Hochstrasser, W. Kaiser, and A. Laubereau, Ed., Springer-Verlag, Berlin, 1982, p 260.

(2) P. Bado, P. H. Berens, J. P. Bergsma, M. H. Coladonato, C. G. Dupuy, P. M. Edelsten, J. D. Kahn, K. R. Wilson, and D. R. Fredkin in "Proceedings of the International Conference on Photochemistry and Photobiology", A. Zewail, Ed., Harwood Academic, New York, in press.

(3) J. R. Reimers, K. R. Wilson, and E. J. Heller, *J. Chem. Phys.*, in press.